Available online at www.sciencedirect.com
SCIENCE DIRECT®
Physics Letters B 595 (2004) 135–142
PHYSICS LETTERS B
www.elsevier.com/locate/physletb

Stability of chiral geometry in the odd–odd Rh isotopes: spectroscopy of ^{106}Rh

P. Joshi, D.G. Jenkins, P.M. Raddon, A.J. Simons, R. Wadsworth, A.R. Wilkinson

Department of Physics, University of York, York, YO10 5DD, UK

D.B. Fossan, T. Koike, K. Starosta [1], C. Vaman

Department of Physics and Astronomy, SUNY, Stony Brook, NY 11794-3800, USA

J. Timár, Zs. Dombrádi, A. Krasznahorkay, J. Molnár, D. Sohler, L. Zolnai

Institute of Nuclear Research, Pf. 51, 4001 Debrecen, Hungary

A. Algora [2]

Instituto de Fisica Corpuscular, CSIC, Universita Valencia, E-46071 Valencia, Spain

E.S. Paul, G. Rainovski [3]

Oliver Lodge Laboratory, Department of Physics, University of Liverpool, L69 7ZE, UK

A. Gizon, J. Gizon

LPSC, 53 avenue des Martyrs, 38026 Grenoble cedex, France

P. Bednarczyk, D. Curien, G. Duchêne

IReS, IN2P3-CNRS/ULP, 23 rue du Loess, 67037 Strasbourg cedex 2, France

J.N. Scheurer

Université de Bordeaux, F-33175 Gradignan cedex, France

Received 11 February 2004; received in revised form 4 May 2004; accepted 25 May 2004

Available online 23 June 2004

Editor: J.P. Schiffer

0370-2693/$ – see front matter
doi:10.1016/j.physletb.2004.05.066

Abstract

The nucleus ^{106}Rh was populated using the reaction ^{96}Zr(^{13}C, p2n) at a beam energy of 51 MeV. γ-ray transitions were identified using the EUROBALL-IV γ-ray spectrometer and the DIAMANT charged particle array. The yrast band, which is based upon a $\pi g_{9/2}^{-1} \otimes \nu h_{11/2}$ configuration, has been extended to $I^{\pi} = (22^{-})$. A new $\Delta I = 1$ band has been identified which resides ~ 300 keV above the yrast band. Core–quasiparticle coupling model calculations show reasonably good agreement with the data. The properties of the two pairs of strongly coupled bands are consistent with a chiral interpretation for these states.

Considerable effort has been made over the last 20 years to obtain conclusive evidence for the existence of triaxial nuclear shapes. These efforts have recently been intensified through the observation of experimental evidence for the existence of chirality in the mass 130 region [1] and the wobbling mode in $A \sim 160$ nuclei [2]. Triaxiality is an essential pre-requisite for the manifestation of both of these effects in atomic nuclei.

The existence of pairs of chiral bands, based on a $\pi h_{11/2} \otimes \nu h_{11/2}^{-1}$ configuration, in odd-odd triaxial nuclei in the $A \sim 130$ region is now well established (e.g., see [1,3–7]). Chirality is a direct consequence of the perpendicular coupling of angular momentum vectors from the odd proton and neutron occupying high-j particle-like and high-j hole-like orbitals, which lie along the short and long axes, respectively, and the triaxial core rotation vector which is oriented along the intermediate axis [8,9]. Theoretically this gives rise to two nearly degenerate $\Delta I = 1$ bands in the laboratory frame, which is one of the key signatures for the formation of chiral geometry in the nuclear intrinsic frame. The symmetry constraints on the wave functions of chiral structures have been investigated and found to have interesting consequences for the electromagnetic properties of the doublet bands which result from the above geometrical arrangement [10]. In particular, staggering in the $B(\mathrm{M1})/B(\mathrm{E2})$ ratios as a function of spin within each band is predicted. The phase of the staggering is found to be related to the parity of the occupied quasiparticle configuration [11]. In addition, a similar staggering, with the same phase, is expected for the ratio of the in-band and out of band M1 transition strengths $(B(\mathrm{M1})_{\mathrm{in}}/B(\mathrm{M1})_{\mathrm{out}})$ for the members of the chiral partner band. Another consequence of chiral geometry is manifested in the form of the constancy of the parameter $S(I)$ (defined as $[E(I) - E(I-1)]/2I$) as a function of spin. This results from the fact that the collective rotation is perpendicular to the angular momenta of both of the odd particles in the chiral geometry. For non-chiral geometry, this would give rise to a large signature splitting, i.e., fluctuations in the $S(I)$ values, in the case of principle axis rotation.

Very recent work on ^{104}Rh [10,12] has provided the first evidence for chirality (and hence triaxiality) based on the $\pi g_{9/2}^{-1} \otimes \nu h_{11/2}$ configuration in the mass 100 region. For this region potential energy surface calculations indicate that ^{106}Rh could provide an even better example of chiral geometry than that found in ^{104}Rh, since the triaxial minimum for the above configuration is predicted to be much closer to -30° (Lund convention) than in ^{104}Rh. It is therefore important to establish whether or not ^{106}Rh possesses similar or even better chiral geometry than ^{104}Rh and indeed to establish whether chirality exists in more than one odd–odd nucleus in this region in order to provide confidence in the structural interpretation.

In the $A \sim 130$ region ^{134}Pr was found to be the only nucleus where degeneracy of the chiral bands was observed. However, the surrounding nuclei were found to exhibit good evidence for the remaining two experimental signatures related to the chiral geometry, i.e., the constancy of the $S(I)$ parameter and the staggering of the $B(\mathrm{M1})/B(\mathrm{E2})$ ratios. It is still an open and interesting question as to whether or not all or indeed any of the above parameters are more robust in the mass 100 region. The present

E-mail address: pj9@york.ac.uk (P. Joshi).

[1] Present address: NSCL, Michigan State University, 164 S. Shaw Lane, East Lansing, MI 48824-1321, USA.

[2] Present address: Institute of Nuclear Research, Pf. 51, 4001 Debrecen, Hungary.

[3] Present address: Department of Atomic Physics, St. Kliment Ohridski The University of Sofia, 5 James Bourchier Blvd, Sofia 1164, Bulgaria.

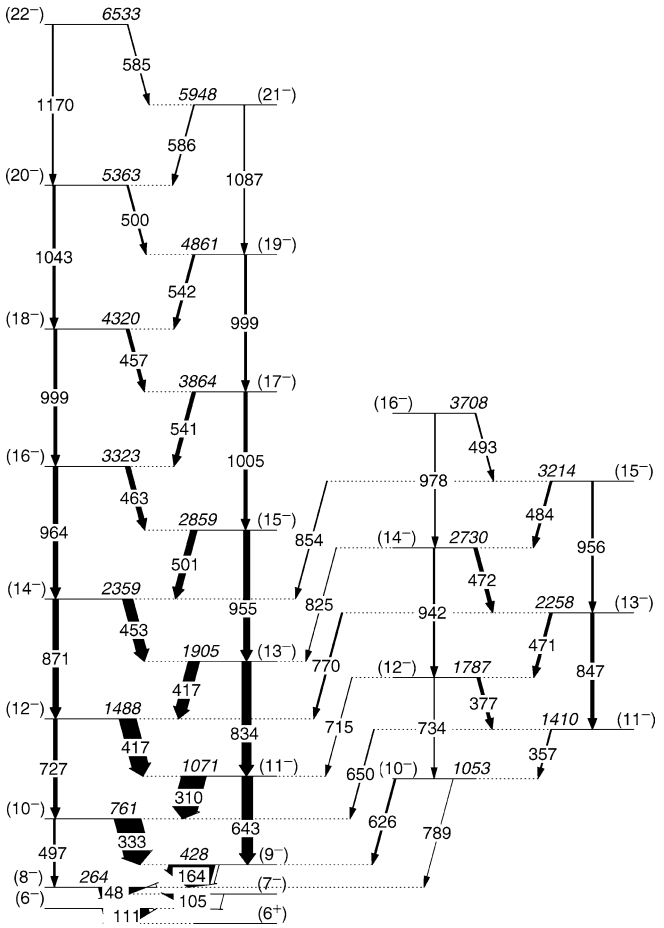

Fig. 1. Partial level scheme for ^{106}Rh obtained in the present work.

work provides experimental evidence for the existence of chiral structures in ^{106}Rh and also presents the first detailed comparison between data and core–quasiparticle coupling calculations in this mass region.

The investigation of excited states in ^{106}Rh presents a difficult experimental challenge since the nucleus can only be populated very weakly in fusion evaporation reactions. The low-lying yrast levels of the nucleus were first identified in fusion–fission work [13,14], where a strongly coupled structure based on the $\pi g_{9/2}^{-1} \otimes \nu h_{11/2}$ configuration was identified up to a spin and parity of (16^-). (Note: the absolute spin values are uncertain since the ground state spin is unknown, however, comparisons with data in other odd–odd Tc, Rh and Ag isotopes [13–20] strongly support the spin assignments made.) In the present work we have used the ^{96}Zr(^{13}C, p2n) fusion–evaporation reaction at a beam energy of 51 MeV to populate excited states in ^{106}Rh. A stack of two (86% enriched) ^{96}Zr targets, each of 590 μg/cm^2, was used in the experiment. The cross-section for the p2n channel is estimated to be 2–4 mb. The EUROBALL-IV [21] array, comprising of only the clover and the cluster Ge detectors, was used in conjunction with the DIAMANT charged particle array [22]. The events associated with the proton channel were identified by gating on a two-dimensional spectrum containing the energy of the detected charged particles along one axis and their PID (particle identification) along the other axis. The PID is an electronically generated signal from the DIAMANT electronics [23] which utilizes a combination of ballistic deficit and zero cross-over timing.

Table 1
γ-ray energies, intensities, directional correlation ratios and linear polarization data for transitions in ^{106}Rh

E_γ	I_γ	Directional correlation ratio (R)	Polarization (P)	Multipolarity
164.4	100(9)	1.02(3)[a]		M1
309.6	52.7(20)	1.05(3)[a]	−0.44(12)	M1
333.1	57.4(23)	1.24(4)[a]	−0.46(16)	M1
357.5	1.6(13)			(M1)
376.7	6.4(18)	1.02(11)[a]		(M1)
416.6	24.3(13)	0.62(10)[b]		M1
417.3	36.7(18)	0.57(5)[b]		M1
453.3	22.5(12)	0.97(5)[a]	−0.35(22)	M1
456.7	6.8(7)	0.85(16)[a]		M1
463.5	10.6(8)	0.97(11)[a]		M1
470.5	5.8(18)	0.90(12)[a]	−0.98(35)	M1
471.5	7.8(23)	0.90(12)[c]	−0.98(35)[c]	M1
484.0	4.4(16)			(M1)
493.0	2.1(24)			(M1)
497.0	3.7(10)			(E2)
500.3	3.3(8)		−0.85(29)	M1
501.0	14.3(11)		−0.85(29)[a]	M1
541.0	7.6(14)	1.07(9)[a]	−0.72(30)	M1
541.7	4.5(13)	1.07(9)[c]	−0.72(30)[c]	M1
585.2	1.7(9)			(M1)
585.7	2.0(9)			(M1)
625.6	3.6(21)	1.15(18)[a]	−0.58(68)	M1/E2
642.9	24.0(9)		1.10(31)	E2
650.0	1.5(9)	1.41(20)[a]	−0.61(64)	M1/E2
715.4	0.6(10)			(M1/E2)
727.2	8.8(9)	1.68(5)[a]	0.98(34)	E2
733.6	0.3(3)			E2
770.2	1.1(4)	1.15(18)[a]		M1/E2
789.0	0.1(7)			
824.8	0.5(12)			(M1)
834.3	20.3(11)	1.77(12)[a]	0.75(30)	E2
847.0	7.6(15)			(E2)
854.0	1.6(16)			(M1/E2)
871.1	12.2(8)	1.68(15)[a]	1.01(37)	E2
941.8	3.8(20)			(E2)
954.6	13.9(9)	1.71(16)[a]		E2
956.0	3.8(14)		0.38(50)	(E2)
963.8	10.4(7)	1.56(16)[a]	0.70(46)	E2
977.6	1.8(21)			(E2)
998.5	5.2(16)	1.99(19)[a]	0.50(25)	E2
998.6	6.8(16)	1.99(19)[c]	0.50(25)[c]	E2
1004.5	7.7(7)	1.82(20)[a]	1.58(32)	E2
1043.2	5.9(6)	1.81(18)[a]		E2
1086.7	2.3(5)			(E2)
1170.3	2.8(5)			(E2)

[a] Gated by stretched dipole.
[b] Gated by stretched quadrupole.
[c] Combined value with previous listed transition of similar energy.

The list mode data were unpacked and sorted into a Radware [24] 3-dimensional cube using the condition that a proton is detected in the DIAMANT array along with each γ-ray event. These data were used to construct the level scheme of ^{106}Rh shown in Fig. 1. The data from the clover and the cluster

detectors also allowed us to deduce the directional correlation (DCO) ratios, R, as well as polarization information for the γ rays in this nucleus. In the EUROBALL-IV geometry the clover and the cluster detectors were arranged at an average angle of 90° and 156° from the beam axis, respectively. The DCO ratio R, is defined as the ratio of the intensity of a transition seen in the cluster detectors when gated by a γ ray in the clover detectors, to the intensity of that transition in the clover detectors when gated by the same γ ray in the cluster detectors. A two-dimensional E_γ–E_γ matrix comprising of the γ rays detected in the cluster detectors along one axis and the γ rays detected in the clover detectors along the other axis was used for this analysis. Investigations of transitions of known multipolarity revealed that a value of $R = 1.0$ is expected if the observed as well as the gating transitions are stretched and have the same multipolarity. Similarly, the values $R = 0.54$ and 1.85 are expected for a stretched dipole transition gated by a stretched quadrupole transition and for a stretched quadrupole transition gated by a stretched dipole transition, respectively. The clover detectors also allowed us to measure the linear polarization of the γ rays [25,26]. For this purpose two γ–γ matrices were constructed. Each of these two matrices had, along one of their axes, the γ rays depositing their full energy with a double hit in the same clover detector while being scattered in a direction perpendicular, or parallel, to the reaction plane, respectively. The other axis in each case contained γ rays detected anywhere in the array. The linear polarization for a γ ray is defined as

$$P = \frac{1}{Q}\frac{N_+ - N_-}{N_+ + N_-}, \tag{1}$$

where N_+ and N_- represent the number of γ rays of a given energy that are scattered in a perpendicular, or parallel, direction to the reaction plane, respectively. Q is the polarization sensitivity, which has an energy dependence and is described in more detail in reference [26]. Positive values of P indicate an electric character while negative values indicate magnetic radiation. The γ ray intensities, DCO ratios (R) and the linear polarization values (P) for some of the transitions of interest are given in Table 1.

In the present work the yrast negative parity band has been extended up to (22^-). In addition, a second strongly coupled band has been identified up to spin (16^-) (see Fig. 1). Fig. 2 shows the γ ray spectrum obtained by gating on the 471/472 keV doublet in coincidence with the 164 and 333 keV transitions. The DCO ratio for the 377 keV γ ray and the DCO and linear polarization data for the 471/472 keV doublet in the side-band are consistent with an M1 assignment. This new band decays through several γ rays which connect it to the levels of the yrast band. Although the linking transitions are weak, it was possible to deduce the DCO ratios for three transitions (626, 650 and 770 keV) and the polarization values for two of them. Whilst the deduced values have relatively large errors, they are consistent with a $\Delta I = 1$ M1/E2 multipolarity with a moderate positive mixing ratio. We note, however, that an M1/E2 transition with $\Delta I = 0$ assignment cannot be ruled out from the directional correlation values. The above results do, however, suggest that the new band has exactly the same configuration as the yrast band, i.e., the quasiparticles occupy exactly the same orbitals in a triaxially deformed potential in the two structures. This is further supported by principal axis cranking (PAC) calculations using a triaxially deformed Woods–Saxon (WS) potential, which reveal that the unfavored signature of the $h_{11/2}$ orbital is found to lie at an excitation energy of ~ 600 keV above the favored signature at $\hbar\omega \sim 0.45$ MeV and to increase with frequency. In contrast the experimental splitting between the two bands is ~ 300 keV (see Fig. 3(a)), indicating that the $h_{11/2}$ neutron still occupies the lowest orbital in the triaxial potential.

The perpendicular coupling of the proton hole and neutron particle would give rise to a chiral doublet if the nucleus attains a triaxial shape. In order to investigate the shape of the mean field in ^{106}Rh, we performed calculations based upon the macroscopic–microscopic formalism [27–29]. Similar calculations have successfully predicted triaxial shapes for the known $N = 75$ chiral cases in the $A = 130$ mass region. Calculations were performed using a triaxial WS potential with Universal parametrization for the mean field and the monopole pairing interaction between pairs of like nucleons as the short range interaction. The calculations were done for a range of $\beta_2 - \gamma$ values and the energy was minimized against the hexadecapole deformation for each $\beta_2 - \gamma$ point. The results of these calculations reveal a γ-soft triaxial ground

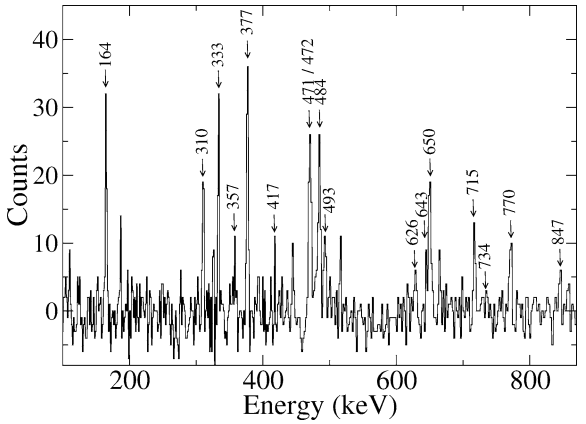

Fig. 2. γ-ray spectrum showing a sum of double coincidences from the cube. The gates used were 471/472 keV doublet γ-ray with the 333 and 164 keV transitions.

state minimum with $\beta_2 \sim 0.23$ and $\gamma \sim -30°$, which persists up to $\hbar\omega > 0.45$ MeV.

As indicated above, recent work in ^{104}Rh [10] provided a detailed theoretical investigation of the experimental conditions necessary for chirality to be observed in nuclei. One of these conditions is that the value of $S(I)$ should be independent of spin for the doublet $\Delta I = 1$ bands. Fig. 3(a) shows that this quantity is essentially constant with spin for the bands in ^{106}Rh. A further fingerprint for chiral structures is the characteristic staggering in the in-band $B(\mathrm{M1})/B(\mathrm{E2})$ ratios as a function of spin. The chiral symmetry imposes certain phase restrictions on the wave functions which relate the nature of this staggering to the spins. The odd spin members of the band should be staggered low compared to the even spins for the negative parity $\pi g_{9/2}^{-1} \otimes \nu h_{11/2}$ configuration. In addition to this, a similar trend is also expected for the $B(\mathrm{M1})_{\mathrm{in}}/B(\mathrm{M1})_{\mathrm{out}}$ ratios for the partner band [11,12]. The phase of the staggering is opposite to that found in the $A = 130$ region, where the chiral states have even parity and therefore, the even spin members are staggered lower compared to the odd ones. Fig. 3(a) shows a plot of the experimental $B(\mathrm{M1})/B(\mathrm{E2})$ and $B(\mathrm{M1})_{\mathrm{in}}/B(\mathrm{M1})_{\mathrm{out}}$ values for the observed bands in ^{106}Rh. The results for these two characteristics are consistent with what is expected from a chiral structure.

It is interesting to note that ^{106}Rh fails to comply with the third characteristic expected for chiral bands, i.e., that it should attain degeneracy at some particular spin. In ^{106}Rh the partner band remains at an almost constant separation of $\sim$300 keV above the yrast band whereas in ^{104}Rh it attains near-degeneracy at spin 17^- [12]. This observation is similar to that found in the mass 130 region where only in ^{134}Pr are the chiral bands found to become degenerate, e.g., see [1,5,6]. This is interesting since ^{106}Rh was expected to possess better chiral geometry than ^{104}Rh because the triaxiality was predicted to be closer to $-30°$. Assuming that the calculations are correct this suggests that better triaxiality is not necessarily indicative of a better degeneracy. One possible reason for the partner bands not to be degenerate is the γ-softness of the mean field, which can give rise to chiral vibrations [1]. In this case, due to the γ-softness of the core, the rotational angular momentum vector does not remain out of the plane (defined by the long and the short axes) all the time but spends some time within the plane as well. If the ^{106}Rh core is more γ-soft than that of ^{104}Rh then these so-called chiral vibrations may explain the lack of degeneracy between the two chiral partners in ^{106}Rh.

In order to further investigate the properties of high spin states in ^{106}Rh, we performed core–quasiparticle coupling calculations [11]. In these calculations, an odd proton in the $g_{9/2}$ orbital and an odd neutron in the $h_{11/2}$ orbital were coupled to a rigid triaxial core. The deformation parameters used for the core were $\beta_2 = 0.235$ and $\gamma = -30°$. These parameters were obtained from the macroscopic–microscopic calculations discussed above. The core's rotational state energies were calculated using the Variable Moment of Inertia (VMI) model, with the value $E(2^+) = 275$ keV used for calculating the ground state moment of inertia. The coupling constant for the particle-rotor quadrupole–quadrupole interaction was determined by reproducing the correct level sequence in the nearby odd A isotopes of Rh. This value of coupling constant (36.2 MeV/b^2) was then used for both protons and neutrons. Monopole pairing was used as the residual interaction between pairs of like nucleons. In addition, a pairing constant $\Delta = 1.237$ MeV was used for both protons and neutrons. This was calculated using the assumption $\Delta = 135/A$. Small changes in Δ did not have any significant effect on the results of the calculations. The Fermi levels for protons and neutrons were fixed to reproduce the correct levels in ^{105}Rh and ^{106}Rh, respectively.

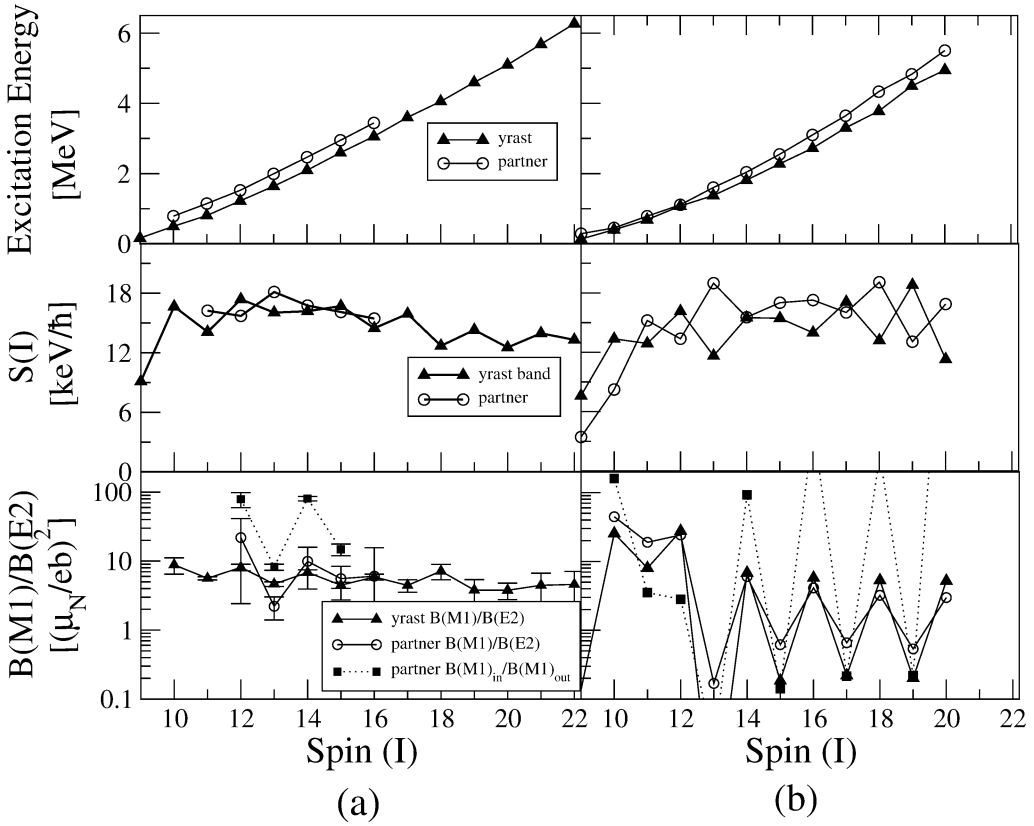

Fig. 3. Plot of the excitation energy (top), staggering $S(I) = [E(I) - E(I-1)]/2I$ (middle) and the $B(\mathrm{M1})/B(\mathrm{E2})$ ratios for the yrast and partner bands as well as the $B(\mathrm{M1})_{\mathrm{in}}/B(\mathrm{M1})_{\mathrm{out}}$ ratios for the partner band (bottom), as a function of spin. These are shown for: (a) experimental data, (b) particle-rotor model calculations. The same symbols have been used for both the experimental and theoretical results.

Fig. 3(b) shows the results of the calculations and their comparison with the data. It is clear from the figure that for a triaxial deformation a chiral geometry exists giving rise to a pair of bands which are separated from each other by 200–300 keV in energy at moderate spins. This is close to the experimental separation between the two bands (~ 300 keV). A more detailed investigation of the calculations shows that at low spins the bands are initially closer together and then start to diverge at around spins 12. (Note, however, the separation between the bands is sensitive to factors such as the moment of inertia used in the calculations.) It is also possible that the near-degeneracy found at low spins in the present calculations may be removed by including a residual p–n interaction, since this would be expected to affect states near the band head more than at higher spins. Unfortunately such calculations cannot be performed at the present time. The near-degeneracy observed around spin 12 in the present calculations is responsible for disturbing the staggering in the $B(\mathrm{M1})_{\mathrm{in}}/B(\mathrm{M1})_{\mathrm{out}}$ values at this point.

The $S(I)$ values for the two calculated bands have no significant spin dependence, which (as discussed above) is an expected characteristic for chiral bands. The experimental and theoretical $S(I)$ values also compare well with each other in their average magnitude. Furthermore, the staggering shown in the plot of the experimental $B(\mathrm{M1})/B(\mathrm{E2})$ values for the two bands although less pronounced, is in reasonable agreement with the calculated values. Both the experimental and the theoretical plots show the same phase for the staggering. Additionally, the experimental $B(\mathrm{M1})_{\mathrm{in}}/B(\mathrm{M1})_{\mathrm{out}}$ values, which are also expected to follow a staggering pattern with the same phase as the $B(\mathrm{M1})/B(\mathrm{E2})$ values, compare favor-

ably in both their phase and relative magnitude. The observed level of agreement between the theoretical calculations and the experimental data provides additional support for the chiral interpretation of the two bands found in ^{106}Rh.

In summary, the nucleus ^{106}Rh was populated using the HI fusion–evaporation reaction ^{96}Zr(^{13}C, p2n) at 51 MeV. The yrast energy level sequence has been extended up to $J^{\pi} = (22^{-})$ while a new strongly coupled band, lying $\sim$300 keV above the yrast band, has been identified up to the (16^{-}) state. These two partner bands possess the characteristic properties expected for a pair of chiral bands. The experimental results compare reasonably well with core–quasiparticle coupling model calculations. The present results, combined with those from the mass 130 region, suggest that achieving energy degeneracy in chiral bands is not a common event. However, the $B(\mathrm{M1})/B(\mathrm{E2})$ and $S(I)$ values observed in ^{106}Rh are found to be very similar to those observed in ^{104}Rh, suggesting that these two quantities are more robust than the energy separation between the chiral bands against fluctuations in the chiral geometry. Further theoretical work is required in order to investigate whether the use of a γ-soft core has any significant effect on the chiral geometry. Such an approach may, for example, be able to explain the near constant separation that is observed for the two bands. Furthermore, the result of adding an p-n residual interaction to calculations of the type presented in this work would also be interesting in order to see how this affects the separation between the two bands at lower spins. The present results support the existence of a new region of chirality in the $Z \sim 45$, $A \sim 105$ mass region.

Acknowledgements

The authors would like to acknowledge the EPSRC in the UK, the European Community—Access to Research Infrastructures action of the Improving Human Potential Programme (contract EUROVIV: HPRI-CT-1999-00078) and the Hungarian Scientific Research Fund, OTKA (contract Nos. T038404, T046901) as well as the Bolyai János Foundation, for the financial support.

References

[1] K. Starosta, et al., Phys. Rev. Lett. 86 (2001) 971.
[2] S.W. Odegard, et al., Phys. Rev. Lett. 86 (2001) 5866.
[3] K. Starosta, et al., Nucl. Phys. A 682 (2001) 375c.
[4] T. Koike, et al., Phys. Rev. C 63 (2001) 061302(R).
[5] A.A. Hecht, et al., Phys. Rev. C 63 (2001) 051302(R).
[6] D. Hartley, et al., Phys. Rev. C 64 (2001) 031304(R).
[7] C.M. Petrache, et al., Nucl. Phys. A 597 (1996) 106.
[8] V. Dimitrov, et al., Phys. Rev. Lett. 84 (2000) 5732.
[9] S. Frauendorf, J. Meng, Nucl. Phys. A 617 (1997) 131.
[10] T. Koike, et al., in: Frontiers of Nuclear Structure, Berkeley, 29 July–2 August, 2002, in: AIP Conf. Proc., vol. 656, American Institute of Physics, New York, 2003, p. 160.
[11] T. Koike, K. Starosta, C.J. Chiara, D.B. Fossan, D.R. LaFosse, Phys. Rev. C 67 (2003) 044319.
[12] C. Vaman, et al., Phys. Rev. Lett. 92 (2004) 032501.
[13] N. Fotiades, et al., Phys. Rev. C 67 (2003) 064304.
[14] M.-G. Porquet, et al., Eur. Phys. J. A 15 (2002) 463.
[15] A. Gizon, et al., Eur. Phys. J. A 2 (1998) 325.
[16] J. Gizon, et al., Nucl. Phys. A 658 (1999) 97.
[17] R. Duffait, et al., Nucl. Phys. A 454 (1986) 143.
[18] J. Tréherne, et al., Phys. Rev. C 27 (1983) 166.
[19] R. Popli, et al., Phys. Rev. C 23 (1981) 1085.
[20] A.M. Bizzeti-Sona, et al., Z. Phys. A 352 (1995) 247.
[21] J. Simpson, Z. Phys. A 358 (1997) 139.
[22] J.N. Scheurer, et al., Nucl. Instrum. Methods A 385 (1997) 501.
[23] J. Gál, et al., Nucl. Instrum. Methods A 516 (2004) 502.
[24] D.C. Radford, Nucl. Instrum. Methods A 361 (1995) 297.
[25] G. Duchene, et al., Nucl. Instrum. Methods A 432 (1999) 90.
[26] P.M. Jones, et al., Nucl. Instrum. Methods A 362 (1995) 556.
[27] W. Nazarewicz, M.A. Riley, J.D. Garrett, Nucl. Phys. A 512 (1990) 61.
[28] T.R. Werner, J. Dudek, At. Data Nucl. Data Tables 59 (1995) 1.
[29] T.R. Werner, J. Dudek, At. Data Nucl. Data Tables 50 (1992) 179.